Electrophysiological Characterization of Membrane Disruption by Nanoparticles

Maurits R. R. de Planque,[†,*] Sara Aghdaei,[†] Tiina Roose,[§] and Hywel Morgan[†,*]

[†]School of Electronics and Computer Science and [§]School of Engineering Sciences, University of Southampton, Southampton SO17 1BJ, United Kingdom

ABSTRACT Direct contact of nanoparticles with the plasma membrane is essential for biomedical applications such as intracellular drug delivery and imaging, but the effect of nanoparticle association on membrane structure and function is largely unknown. Here we employ a sensitive electrophysiological method to assess the stability of protein-free membranes in the presence of silica nanospheres of different size and surface chemistry. It is shown that all the silica nanospheres permeabilize the lipid bilayers already at femtomolar concentrations, below reported cytotoxic values. Surprisingly, it is observed that a proportion of the nanospheres is able to translocate over the pure-lipid bilayer. Confocal fluorescence imaging of fluorescent nanosphere analogues also enables estimation of the particle density at the membrane surface; a significant increase in bilayer permeability is already apparent when less than 1% of the bilayer area is occupied by silica nanospheres. It can be envisaged that higher concentrations of nanoparticles lead to an increased surface coverage and a concomitant decrease in bilayer stability, which may contribute to the plasma membrane damage, inferred from lactate dehydrogenase release, that is regularly observed in nanotoxicity studies with cell cultures. This biophysical approach gives quantitative insight into nanosphere–bilayer interactions and suggests that nanoparticle–lipid interactions alone can compromise the barrier function of the plasma membrane.

KEYWORDS: silica nanoparticles · lipid bilayers · membranes · electrophysiology · nanobiophysics · nanotoxicology

Cellular uptake of nanoparticles is a prerequisite for nanomedical applications such as targeted drug delivery and subcellular imaging. Nanoparticle uptake is generally considered to be an active process, mediated by membrane proteins that facilitate encapsulation of membrane-associated nanoparticles into an intracellular vesicle with a particular subcellular destination,[1,2] although passive uptake may occur as well.[3] A point of concern is that the required contact of the nanoparticles with the cell membrane also carries the risk of membrane disruption and cytotoxic effects. Indeed, lactate dehydrogenase (LDH) release from cells, a biochemical assay for plasma membrane damage, has been observed for a wide range of nanoparticles.[4] Despite an intensive research effort, it remains uncertain how physicochemical properties such as nanoparticle size, shape, and surface chemistry relate to the extent of membrane disruption or to nanoparticle-induced cytotoxicity in general. Consequently there is at present no firm scientific basis for the safety and risk assessment of nanomaterials.[5,6]

Direct comparison of nanotoxicology studies is complicated by the considerable variation in cell lines, suspension media, and assay conditions and also by lack of characterization of the aggregation state and effective concentration of the nanoparticles. Systematic studies include the work by Napierska *et al.*, who investigated the viability of endothelial cells in the presence of monodisperse silica nanospheres with seven different diameters (ranging from 14 to 335 nm): LDH and mitochondrial activity assays demonstrated that a reduction in diameter leads to an increase in toxicity.[7] In general, a picture is emerging that smaller nanoparticles, with a diameter of tens of nanometers or less, are consistently more toxic than larger analogues, with a diameter of hundreds of nanometers.[6] For particles of the same size, it has also been observed that cationic particles are more toxic than net neutral analogues or anionic analogues, which could reflect an increased affinity for association with the (negatively charged) plasma membrane.[6,8]

As a complementary development, various groups have sought to gain insight into the mechanism of nanoparticle-induced cytotoxicity, specifically membrane damage, by employing model membrane systems (lipid bilayers). A key feature of these is that particle aggregation and protein adsorption, which lead to an unknown effective diameter or surface chemistry, can be avoided because there is no requirement to disperse the particles in cell culture medium.[9–11] Examples of such biophysical approaches include the surface pressure analysis of lipid displacement from lipid

* Address correspondence to mdp@ecs.soton.ac.uk, hm@ecs.soton.ac.uk.

Received for review December 5, 2010 and accepted April 25, 2011.

Published online April 25, 2011
10.1021/nn103320j

monolayers by functionalized polystyrene nanospheres, atomic force microscopy imaging of defects in supported lipid bilayers exposed to various cationic particles, spectroscopic detection of nanotube-triggered release of an encapsulated dye from pure-lipid vesicles, and surface charge-dependent bilayer translocation of gold nanoparticles in a coarse-grained simulation model.[12−15] All these studies suggest that nanoparticles are able to perturb the structure of protein-free membranes.

In the present study we use electrophysiology, the most sensitive method to evaluate membrane permeability, to measure nanoparticle-induced ion flow over lipid bilayers. It is shown that monodisperse spherical silica nanoparticles, which are under development for intracellular drug delivery[16,17] but are known to be cytotoxic at higher concentrations,[7] degrade the barrier function of sterol-free and sterol-containing bilayers. The measured increase in membrane permeability depends on nanosphere concentration, surface chemistry, and size. Fluorescence imaging shows that the nanospheres are enriched at the lipid−water interface and are able to translocate across the bilayer. This sensitive biophysical approach gives quantitative insight into the affinity of the nanoparticles for the membrane. To the best of our knowledge, this is the first study in which the extent of nanoparticle-induced membrane perturbation has been correlated with the nanoparticle density at the membrane surface.

RESULTS AND DISCUSSION

Lipid bilayers were formed using the droplet-in-oil methodology recently developed by Takeuchi and Bayley.[18,19] Two droplets of aqueous KCl solution were submerged into a lipid-containing oil phase (decane), enabling the self-assembly of a lipid monolayer at the water−oil interface of each droplet. An exceptionally stable bilayer can be formed when the two droplets are subsequently brought into contact. Droplet position and droplet−droplet contact force were precisely controlled with electrodynamic (dielectrophoresis) forces generated using a planar microelectrode structure developed in our group.[20] As depicted in Figure 1, an Ag|AgCl electrode was inserted into each droplet to enable bilayer capacitance measurements and electrical bilayer recordings with single ion channel sensitivity. Bilayers were made from 1,2-dioleoyl-*sn*-3-phosphatidylcholine (DOPC), a synthetic lipid extensively used for membrane permeabilization studies of membrane-degrading compounds such as bacterial toxins and antimicrobial peptides,[21] or from asolectin, a natural lipid extract that, like mammalian plasma membranes, includes sterols that render the membrane more rigid.[22] For both lipid compositions, a stable current of typically 5 pA with a peak-to-peak noise of ∼6 pA was measured at an applied dc voltage of +100 mV (Figure 2a,d,g). The low baseline current

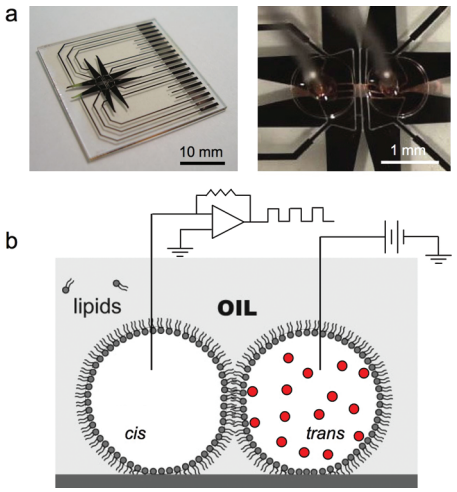

Figure 1. Microelectrode array and schematic diagram for electrophysiology with water-in-oil droplets. Aqueous droplets that are introduced into an oil phase containing solubilized lipids become coated with a lipid monolayer. (a) Two lipid-coated droplets are brought into contact by dielectrophoretic manipulation on a 16 × 16 mm platinum microelectrode array as described in ref 20. (b) Where the two droplets are in physical contact, the oil is expelled and an extremely stable lipid bilayer is formed. After placing Ag|AgCl electrodes into each droplet from above, the bilayer is voltage-clamped at +100 mV and the bilayer current is monitored with single ion-channel sensitivity, in the absence and presence of nanoparticles in the *trans* droplet, which mimicks the extracellular environment.

confirms the formation of an electrically insulating membrane with a gigaohm resistance. The typical capacitance of these bilayers was ∼300 pF, which, given a specific capacitance of 0.5 μF/cm^2, is equivalent to a lipid bilayer with a surface area of 0.06 mm^2.[20,23] In the absence of nanoparticles, the interdroplet bilayers are stable for several hours, up to ∼20 h in the case of asolectin,[20] with no changes in the bilayer current.

Nanosphere-Induced Bilayer Current. For DOPC bilayers, when one of the two microdroplets contains ∼10 000 silica nanospheres with a nominal diameter of 500 nm and $-NH_3^+$ surface functionalization, the bilayer current rapidly reaches ∼50 pA, followed by a steady increase to ∼100 pA over approximately three minutes, and then jumps to >300 pA (Figure 2b), at which point the bilayer disintegrates. This implies that at this relatively low concentration (∼8 fM; 0.62 μg/mL), these nanospheres render the DOPC bilayer increasingly permeable to ions and destabilize it to such an extent that the bilayer lifetime is severely reduced. At a 1000-fold higher nanoparticle concentration of ∼8 pM (620 μg/mL), the gradually increasing bilayer current is characterized by bursts of short (2−5 ms duration) current spikes, up to ∼200−250 pA, and the DOPC bilayer collapses already after ∼90 s (Figure 2c). In contrast, for the more rigid asolectin bilayers, the current baseline remains constant for approximately 15−30 min, which is sufficiently long for routine electrophysiology measurements. An increase in

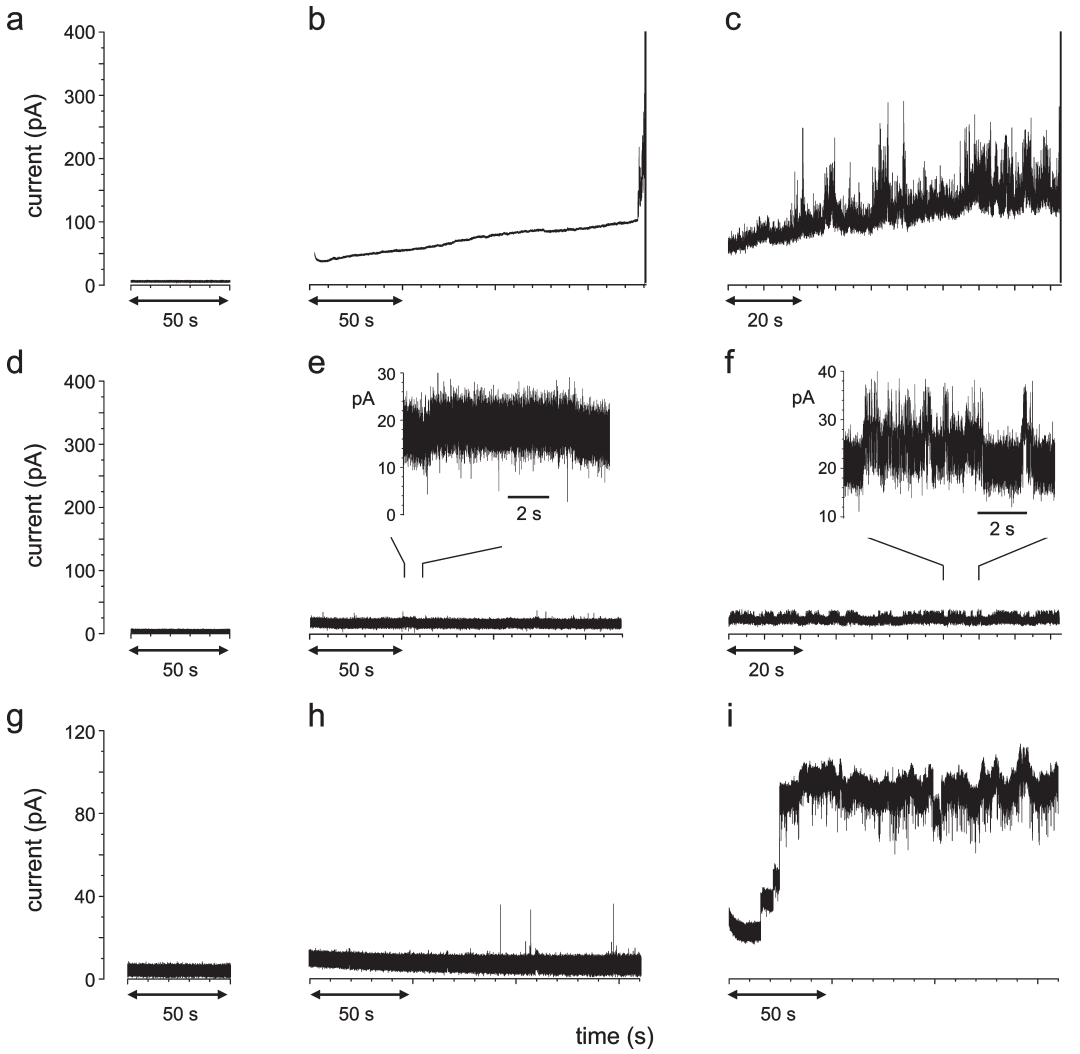

Figure 2. Current measurements of voltage-clamped bilayers of DOPC and asolectin in the absence and presence of nanoparticles. (a−c) DOPC bilayer exposed to 500 nm aminated silica nanospheres: (a) 0 fM, (b) 8 fM, (c) 8 pM. (d−f) Asolectin bilayer exposed to 500 nm aminated silica nanospheres: (d) 0 fM, (e) 8 fM, (f) 8 pM. (g−i) Asolectin bilayer in the presence of different nonfunctionalized silica nanospheres with the same total surface area: (g) no nanoparticles, (h) 500 nm silica nanospheres at 8 fM concentration, and (i) 50 nm silica nanospheres at 1 pM concentration. The droplets were approximately 2 μL of 100 mM KCl solution, with nanoparticles in the *trans* droplet.

asolectin bilayer current, up to ~20 pA, and current spikes of up to ~35 pA (0.5−1.0 ms duration) are observed at the higher nanoparticle concentration (Figure 2e,f). For both the DOPC and asolectin lipid bilayers, the reduced lifetime and the increase in bilayer current clearly indicate that the aminated nanospheres have a membrane-disrupting effect. It should also be noted that current−voltage relationships for asolectin bilayers in the presence of silica nanospheres are linear between −100 and +100 mV. Such ohmic behavior implies the presence of pores, channel-like structures or lipid packing defects, with a diameter that exceeds ~2 nm.[24] To rule out the possibility that the bilayer perturbation is induced by surfactants or other dispersion-stabilizing molecules in the nanoparticle stock solution, we investigated the effect of the suspending medium itself, after removal of the nanoparticles (see Methods). Even though the same amount of medium was present as would have been the case for a high nanoparticle concentration of 68 pM, the steady-state DOPC bilayer current was negligible (<5 pA for over 30 min; data not shown), demonstrating that the bilayer current events (*e.g.*, Figure 2b,c) are caused by the nanoparticles themselves. As a point of reference, it has recently been reported that 500 nm aminated silica particles at ~50 μg/mL concentration decrease the viability of cell cultures;[25] our experiments show that at concentrations 100 times below this the particles already act as potent bilayer disruptors.

The only previous electrophysiological studies, to our knowledge, show that also CdSe quantum dots of 3−15 nm diameter cause current bursts of up to 800 pA (8 nS) in DOPC-containing bilayers and channel-like current spikes of up to 30 pA (0.6 nS) in more rigid bilayers of diphytanoyl phosphatidylcholine.[26,27] Additionally, Chen *et al.* recently demonstrated that

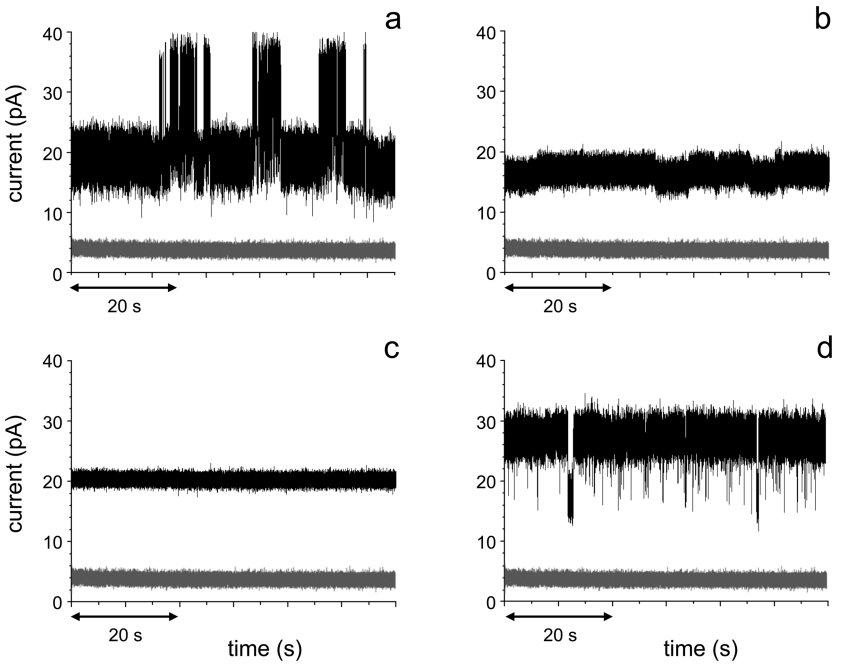

Figure 3. Current measurements of voltage-clamped bilayers of asolectin in the presence of (a) 500 nm diameter aminated silica nanospheres, (b) 50 nm aminated nanospheres, (c) 500 nm nonfunctionalized silica nanospheres, (d) 50 nm nonfunctionalized nanospheres. The silica nanospheres were present at a concentration of 5 million particles per microliter (8 pM) in 10 mM KCl. The gray traces in each panel depict the bilayer current in the absence of nanoparticles.

various cationic polymer nanoparticles (~5−8 nm diameter) gradually increase the conductance of cell membranes, with occasional discrete current steps of up to 0.9 ± 1.2 nA, as measured by patch-clamp electrophysiology of living cells.[28] A key difference with these polymeric nanoparticles and quantum dots is the larger diameter and the larger variation in diameter of the silica nanospheres investigated here. The larger size is likely to give rise to different particle−membrane interaction mechanisms, while the larger range in sizes complicates the comparison of different particles. Figure 2h shows that 500 nm nonfunctionalized silica particles at a concentration of 5000 particles/μL (8 fM) give rise to a similar increase in bilayer current as the 500 nm aminated nanospheres at this concentration (Figure 2e), whereas 50 nm nonfunctionalized nanospheres at a 100-fold higher molar concentration (note the similar total particle surface area of ~4−6 mm^2/mL (Table S1 in the Supporting Information)) cause a substantially increased bilayer current of ~100 pA (Figure 2i). This observation indicates that it is more meaningful to compare the effect of nanospheres of different size at the same molar concentration than at the same total surface area.

Effect of Nanosphere Size and Surface Charge on Bilayer Permeability. To investigate whether the size and/or the surface chemistry of the silica nanospheres modulates the interactions with the bilayer, we measured the bilayer current in the presence of a small set of silica nanospheres that differ in nominal diameter (50 or 500 nm) and surface chemistry (plain or amine-functionalized silica). The nanospheres were diluted in 10 mM KCl to reduce any salt screening effects that could lead to particle clustering.[29] Figure 3 shows the effect of the different nanoparticles at picomolar concentration: the bilayer current for all the nanospheres is substantially higher, often exceeding 20 pA, than for the bilayer in the absence of nanoparticles. Except for the 500 nm diameter nonfunctionalized silica nanospheres, all the particles also induce current spikes (1−4 ms duration) and/or current steps (>20 ms duration), with a frequency of ~1−10 events per second. Interestingly, these current transitions frequently occur with a relatively well-defined amplitude, as highlighted in Figure 4 by applying a 50 Hz low-pass filter. Interestingly, similar "ion channel-like" modulation of the bilayer current has also been observed for cytotoxic β-amyloid oligomers,[30,31] which may suggest that silica nanospheres and nanoscale amyloid aggregates interact with lipid bilayers through a related mechanism.

As judged from the maximum intensity of the bilayer current and the peak-to-peak baseline current (Figure 3), the bilayer-disrupting effect of the silica nanospheres is most pronounced for the 500 nm aminated particles, whereas the 500 nm particles with a nonfunctionalized silica surface have the smallest effect. However, the 50 nm nonfunctionalized silica nanospheres appear more disruptive than the aminated analogues of the same diameter. Our electrophysiology data thus imply that neither the size nor the surface chemistry of these nanospheres dominates the

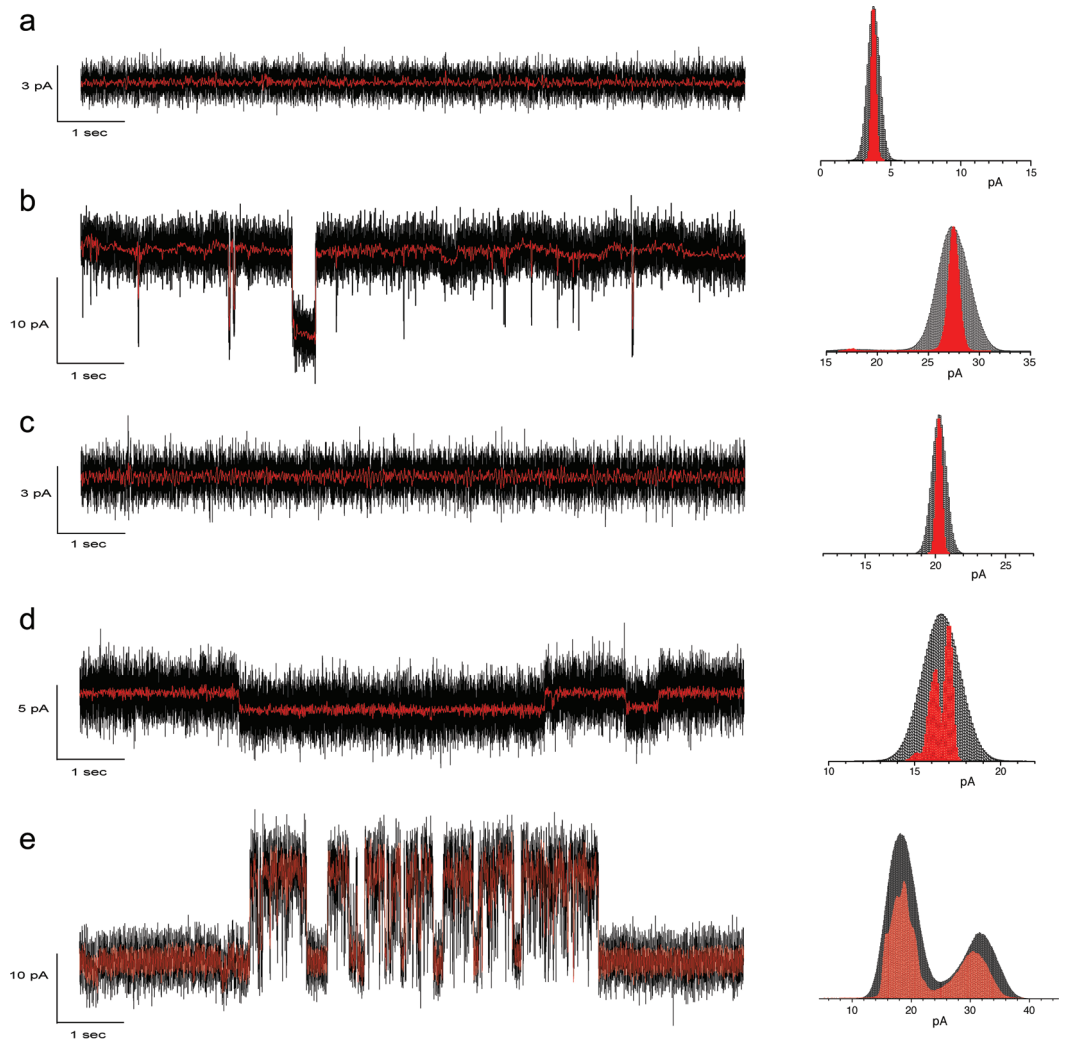

Figure 4. Expanded view of asolectin bilayer current trace and histogram of current distribution for the following silica nanospheres: (a) no nanoparticles, (b) 50 nm nonfunctionalized particles, (c) 500 nm nonfunctionalized particles, (d) 50 nm aminated particles, (e) 500 nm aminated particles. The nanosphere concentration is 8.3 pM in 10 mM KCl. A 50 Hz low-pass filter (red traces) was applied to emphasize the well-defined amplitude of the current steps in the unfiltered data (black traces). The histograms are for current traces with a duration of 60 s (50 Hz low-pass filtered data are shown in red).

interaction with the overall negatively charged asolectin bilayer. Experiments with bilayers with various charge densities and with a larger set of nanoparticles could give insight into the apparent interplay of size and surface chemistry effects. In other studies with silica nanospheres in aqueous buffer solution rather than cell culture medium, 50 nm aminated silica nanospheres were found to cause the formation of ~100 nm holes in mica-supported phosphatidylcholine bilayers at nanomolar particle concentration.[13] Very recently, nonfunctionalized silica nanospheres with diameters of 37, 142, and 263 nm have been shown to induce 50% lysis of isolated red blood cells at concentrations respectively of 18 μg/mL (515 pM), 94 μg/mL (47 pM), and 307 μg/mL (25 pM).[32] Our investigation of asolectin bilayers, the sterol content of which is comparable to the red blood cell membrane,[22] demonstrates that 50 and 500 nm diameter silica nanospheres already cause a significant increase in bilayer current at a concentration of 8 pM, highlighting the sensitivity of electrophysiological characterization of membrane permeability.

Localization of Nanospheres at the Membrane Surface. The nanoparticle distribution inside the droplets can be visualized with optical microscopy, which enables the number of particles at the membrane surface to be estimated. Aqueous droplets without or with fluorescently labeled nanoparticles were submerged in decane, and the center of the droplets was imaged by confocal fluorescence microscopy. Figure 5 shows that fluorescent nanospheres (500 nm diameter, aminated) cause an increase in fluorescence intensity at the droplet perimeter, but only when asolectin lipids were present in the oil phase, indicating that these nanoparticles have a tendency to associate with the lipids. From the fluorescence intensity profile we estimate that ~5% of the nanospheres is located at the droplet surface, giving a coverage of ~7 $\times$ 10^4

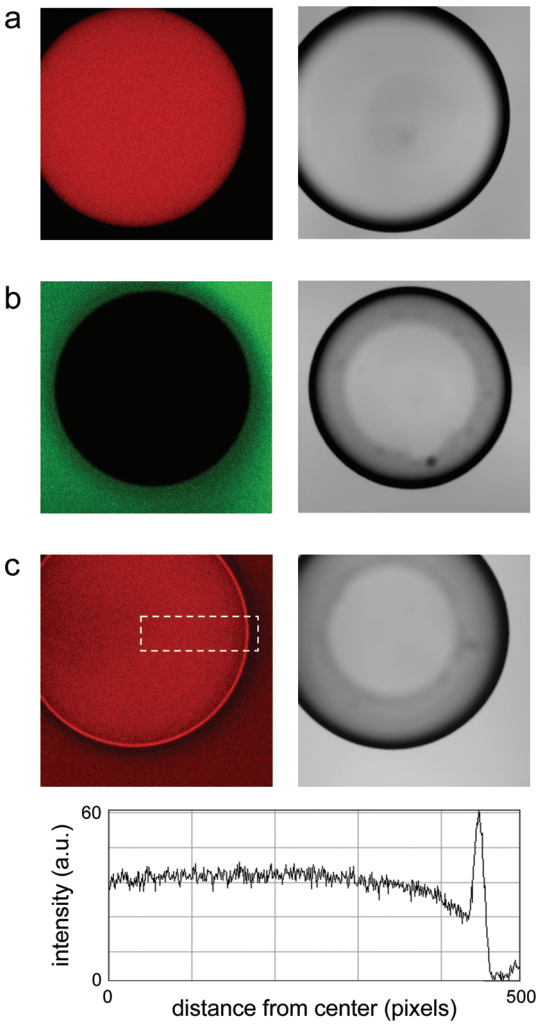

Figure 5. Visualization of the nanosphere distribution in a water-in-oil droplet. Confocal fluorescence images of a droplet of (a) 500 nm diameter fluorescently labeled aminated silica nanospheres in pure decane, (b) 10 mM KCl solution in decane with asolectin lipids, (c) nanospheres (58 pM in 10 mM KCl) in decane/asolectin with fluorescence intensity profile from boxed area. Asolectin has some fluorescent components that have the same false color in panel c as the fluorescent nanospheres. The nanospheres are homogeneously distributed throughout the droplet when it is immersed in pure decane but accumulate at the droplet–decane interface when asolectin lipids are present. Left-side panels are fluorescence images, and right-side panels are transmitted light images. Frames are 1200 × 1200 μm.

particles/mm^2, which for a 0.06 mm^2 bilayer (see above) would imply that the bilayer currents shown in Figures 3 and 4 are caused by ~4 × 10^3 particles. As a point of reference, Cho *et al.* reported association of ~100 cationic gold nanoparticles (18 nm diameter) with the membrane surface of a single cancer cell after one hour of incubation at 27 pM nanoparticle concentration; assuming a cell diameter of 20 μm, this equates to ~1 × 10^5 particles/mm^2.[3] For the silica nanospheres, the estimated nanoparticle density, which represents 2% coverage of the bilayer area in the case of the 500 nm particles and just 0.02% in the case of the 50 nm nanospheres, suggests that the observed increase in bilayer current is a collective effect resulting from the bilayer interactions of a large number of particles. However, the single channel-like current transitions (Figure 4) are likely to be caused by individual particles. Calculations of the mean free path of the particles in three dimensions (see Supporting Information) indicate that at a particle concentration of 8 pM fewer than 10 nanospheres diffuse into a 0.06 mm^2 lipid bilayer area every second (Figure S1 and Table S2). Since this is consistent with the observed frequency of the channel-like current transitions, it seems likely that the current spikes and steps are a result of nanoparticle–bilayer collisions.

Bilayer Translocation. To assess whether lipid association of the nanospheres leads to translocation across the interdroplet bilayer, we investigated the originally empty *cis* droplet (Figure 1b) by optical microscopy. Two 2 μL aqueous droplets were brought together, one with and one without fluorescently labeled aminated nanospheres of 500 nm diameter. The bilayer current was recorded, and then the two droplets were separated, pipetted onto glass slides, and dried out. A series of fluorescence and brightfield microscopy images was taken, covering the entire area of the dried-out *cis* droplet. It was found that a small fraction of the particles, ~0.01–0.05% of the total number of nanoparticles used in these experiments, was present in the *cis* droplet and had thus translocated across the bilayer from the *trans* droplet. This is a significant amount because 0.17% is the theoretical maximum percentage of translocated particles when it is assumed that, during a 30 min measurement, diffusion into the bilayer leads to immediate translocation (Table S3). Since the protein-free membrane employed in this study cannot facilitate active transport, the observed nanosphere translocation was solely a result of passive transport.[1] A mechanism of passive uptake of silica nanoparticles has recently been identified by Le Bihan *et al.*, who showed by cryo-TEM that 100 nm diameter nonfunctionalized silica nanospheres become associated with the surface of DOPC vesicles, induce bilayer invagination, and end up as bilayer-coated nanospheres inside the vesicle.[33] Passive uptake of nanomaterials has also been observed for gold nanoparticles[3] and may occur in parallel with active uptake processes,[1] which are readily identified by fluorescence microscopy because of the enrichment of fluorescently labeled particles in endosomal vesicles.

CONCLUSION

Our electrophysiology and fluorescence study shows that silica nanospheres adsorb to pure-lipid membranes and compromise their structural integrity already at a membrane surface coverage as low as approximately 0.02%. To the best of our knowledge, this is the first time that measurements of the

membrane permeability have been correlated with the number of membrane-associated nanoparticles. Interestingly, Granick and co-workers demonstrated that 20 nm aminated and carboxylated polystyrene nanospheres modulate the physical state of phosphatidylcholine bilayers, inducing localized gel-to-fluid or fluid-to-gel phase transitions,[34,35] implying strong interactions of negatively and positively charged nanospheres with a net uncharged membrane. In the case of the silica nanospheres investigated in the present study, we hypothesize that the tight lipid association typically reported for bilayer-coated silica particles[36−39] causes localized phase changes in the DOPC and asolectin bilayers, analogous to the curvature-dependent shift in the phase transition temperature of silica nanosphere-supported phosphatidylcholine bilayers.[40] These localized phase variations could give rise to transient lipid packing defects[41,42] that are manifested in electrical recordings as an increase in the average bilayer current at picomolar to femtomolar nanoparticle concentrations. It can be envisaged that higher concentrations lead to an increased membrane surface coverage and more severe membrane disruption, as observed in topography imaging of supported lipid bilayers and hemoglobin leakage assays of isolated red blood cells.[13,32] Loss of plasma membrane integrity as assessed by the LDH assay for cells exposed to (silica) nanoparticles[4,7] may thus to some extent be a direct consequence of nanoparticle association with the membrane. Biophysical approaches such as the droplet-based bilayer system complement traditional cell culture studies on the molecular basis of nanotoxic effects and may facilitate high-throughput prescreening of membrane-disruptive nanoparticles.

METHODS

Nanoparticles. Silica nanospheres with nominal diameters of 50 and 500 nm were obtained from G. Kisker GbR (Steinfurt, Germany), either with a plain silica surface or with an amine-functionalized surface. Analogues with a covalently bound dye, with excitation and emission maxima at 569 and 585 nm, respectively, were also from Kisker. The particles were diluted from 25 to 50 mg/mL stock solutions (nanoparticles in surfactant-free (personal communication from manufacturer) deionized water) in 10 or 100 mM KCl. The nanospheres are insoluble in decane.

Nanoparticle Characterization. The hydrodynamic radius of the silica nanospheres was verified with a Zetasizer Nano ZS dynamic light scattering system with a 633 nm laser (Malvern Instruments, Malvern, United Kingdom). Nanosphere dispersions in 10 mM KCl were measured with a 173° backscatter angle in polystyrene cuvettes at 25 °C. Measurements consisted of multiple runs with a total duration of 60−70 s. Data were analyzed by cumulants analysis using Malvern software version 6.01. The polydispersity index of all the particles was below 0.1. The hydrodynamic diameter of the two different nonfunctionalized silica nanospheres was 61 and 462 nm (nominally 50 and 500 nm), and the diameter of the two different aminated silica nanospheres was 61 and 490 nm (nominally 50 and 500 nm).

Droplet Dielectrophoresis. A planar microelectrode array (see Figure 1) was used to move two aqueous droplets together for the reproducible formation of interdroplet lipid bilayers. The 16 × 16 mm array consists of pairs of individually addressable, thin-film, platinum electrodes, patterned using standard photolithographic techniques on a glass substrate. The electrodes were coated with a 0.7 μm insulating layer of the photoresist SU8 to prevent electrochemical reactions. A plastic reservoir was bonded to the surface of the device to contain the lipid−decane solution, and the electrodes were connected to an ac frequency generator and amplifier. By applying a low-frequency electric field between selected microelectrodes, droplets (initially positioned by pipetting) can be moved together by electrodynamic forces, as described in ref 20.

Electrophysiology. Ag|AgCl electrodes were connected to a high-sensitivity ID562 amplifier (Industrial Developments Bangor, Bangor, United Kingdom) and placed in each aqueous droplet (2 μL) to enable capacitance measurements and electrical recordings of the interdroplet lipid bilayer. The *cis* electrode is voltage-controlled, and the *trans* electrode is held at virtual ground. The bilayer current was recorded at a sampling rate of 10 kHz, typically at +100 mV. Unless otherwise noted, unfiltered data are presented. For nanoparticle experiments, one droplet (*trans*) contained nanoparticles at the desired concentration, while the other droplet (*cis*) was pure salt solution. Depicted traces, recorded between 5 and 20 min after the droplets had been brought into contact with each other, are representative data for at least three independent measurements. As a control experiment to test for the absence of surfactants in the nanoparticle stock solution, 0.5 mL of the stock solution of 500 nm aminated particles (50 mg/mL) was centrifuged to separate the particles from the suspending medium (deionized water). Of the clear supernatant fraction, 120 μL was added to 1 mL of a 100 mM KCl solution in a Delrin bilayer cup with a 150 μm diameter aperture (CD13A-150, Warner Instruments, Holliston, MA) with a decane-suspended bilayer of DOPC, and the bilayer current was recorded for over 30 min at +100 mV using Ag|AgCl electrodes connected to the ID562 amplifier.

Microscopy. Confocal fluorescence images of the central plane of a droplet were taken with a Zeiss LSM5 Exciter microscope using a 543 nm laser for the nanoparticle-containing samples and a 488 nm laser for the asolectin/decane control sample. Nanoparticles were used at a higher concentration, 58 pM in 10 mM KCl, to facilitate imaging. Fluorescence intensity profiles were generated by ImageJ software.

Acknowledgment. M.d.P. acknowledges the financial support of the Adventures in Research Grant Scheme (University of Southampton), and T.R. acknowledges the award of the Royal Society University Research Fellowship.

Supporting Information Available: Calculation of nanosphere surface area, diffusion properties, and bilayer flux. This material is available free of charge *via* the Internet at http://pubs.acs.org.

REFERENCES AND NOTES

1. Unfried, K.; Albrecht, C.; Klotz, L. O.; Von Mikecz, A.; Grether-Beck, S.; Schins, R. P. F. Cellular Responses to Nanoparticles: Target Structures and Mechanisms. *Nanotoxicology* **2007**, *1*, 52–71.
2. Slowing, I.; Trewyn, B. G.; Lin, V. S. Y. Effect of Surface Functionalization of MCM-41-Type Mesoporous Silica Nanoparticles on the Endocytosis by Human Cancer Cells. *J. Am. Chem. Soc.* **2006**, *128*, 14792–14793.
3. Cho, E. C.; Xie, J.; Wurm, P. A.; Xia, Y. Understanding the Role of Surface Charges in Cellular Adsorption versus

Internalization by Selectively Removing Gold Nanoparticles on the Cell Surface with a I_2/KI Etchant. *Nano Lett.* **2009**, *9*, 1080–1084.
4. Lewinski, N.; Colvin, V.; Drezek, R. Cytotoxicity of Nanoparticles. *Small* **2008**, *4*, 26–49.
5. Fadeel, B.; Garcia-Bennett, A. E. Better Safe than Sorry: Understanding the Toxicological Properties of Inorganic Nanoparticles Manufactured for Biomedical Applications. *Adv. Drug Delivery Rev.* **2010**, *62*, 362–374.
6. Nel, A. E.; Mädler, L.; Velegol, D.; Xia, T.; Hoek, E. M. V.; Somasundaran, P.; Klaessig, F.; Castranova, V.; Thompson, M. Understanding Biophysicochemical Interactions at the Nano-Bio Interface. *Nat. Mater.* **2009**, *8*, 543–557.
7. Napierska, D.; Thomassen, L. C. J.; Rabolli, V.; Lison, D.; Gonzalez, L.; Kirsch-Volders, M.; Martens, J. A.; Hoet, P. H. Size-Dependent Cytotoxicity of Monodisperse Silica Nanoparticles in Human Endothelial Cells. *Small* **2009**, *5*, 846–853.
8. Xia, T.; Kovochich, M.; Liong, M.; Zink, J. I.; Nel, A. E. Cationic Polystyrene Nanosphere Toxicity Depends on Cell-Specific Endocytic and Mitochondrial Injury Pathways. *ACS Nano* **2008**, *2*, 85–96.
9. Schulze, C.; Kroll, A.; Lehr, C. M.; Schäfer, U. F.; Becker, K.; Schnekenburger, J.; Isfort, C. S.; Landsiedel, R.; Wohlleben, W. Not Ready to Use—Overcoming Pitfalls When Dispersing Nanoparticles in Physiological Media. *Nanotoxicology* **2008**, *2*, 51–61.
10. Clift, M. J.; Bhattacharjee, S.; Brown, D. M.; Stone, V. The Effects of Serum on the Toxicity of Manufactured Nanoparticles. *Toxicol. Lett.* **2010**, *198*, 358–365.
11. Maiorano, G.; Sabella, S.; Sorce, B.; Brunetti, V.; Malvindi, M. A.; Cingolani, R.; Pompa, P. P. Effects of Cell Culture Media on the Dynamic Formation of Protein-Nanoparticle Complexes and Influence on the Cellular Response. *ACS Nano* **2010**, *4*, 7481–7491.
12. Peetla, C.; Labhasetwar, V. Effect of Molecular Structure of Cationic Surfactants on Biophysical Interactions of Surfactant-Modified Nanoparticles with a Model Membrane and Cellular Uptake. *Langmuir* **2009**, *25*, 2369–2377.
13. Leroueil, P. R.; Berry, S. A.; Duthie, K.; Han, G.; Rotello, V. M.; McNerny, D. Q.; Baker, J. R., Jr.; Orr, B. G.; Holl, M. M. B. Wide Varieties of Cationic Nanoparticles Induce Defects in Supported Lipid Bilayers. *Nano Lett.* **2008**, *4*, 420–424.
14. Hirano, A.; Uda, K.; Maeda, Y.; Akasaka, T.; Shiraki, K. One-Dimensional Protein-Based Nanoparticles Induce Lipid Bilayer Disruption: Carbon Nanotube Conjugates and Amyloid Fibrils. *Langmuir* **2010**, *26*, 17256–17259.
15. Lin, J.; Zhang, H.; Chen, Z.; Zheng, Y. Penetration of Lipid Membranes by Gold Nanoparticles: Insights into Cellular Uptake, Cytotoxicity, and Their Relationship. *ACS Nano* **2010**, *4*, 5421–5429.
16. Vivero-Escoto, J. L.; Slowing, I. I.; Wu, C. W.; Lin, V. S. Y. Photoinduced Intracellular Controlled Release Drug Delivery in Human Cells by Gold-Capped Mesoporous Silica Nanosphere. *J. Am. Chem. Soc.* **2009**, *131*, 3462–3463.
17. Park, J. H.; Gu, L.; von Maltzahn, G.; Ruoslahti, E.; Bhatia, S. N.; Sailor, M. J. Biodegradable Luminescent Porous Silicon Nanoparticles for *In Vivo* Applications. *Nat. Mater.* **2009**, *8*, 331–336.
18. Funakoshi, K.; Suzuki, H.; Takeuchi, S. Lipid Bilayer Formation by Contacting Monolayers in a Microfluidic Device for Membrane Protein Analysis. *Anal. Chem.* **2006**, *78*, 8169–8174.
19. Bayley, H.; Cronin, B.; Heron, A.; Holden, M. A.; Hwang, W. L.; Syeda, R.; Thompson, J.; Wallace, M. Droplet Interface Bilayers. *Mol. BioSyst.* **2008**, *4*, 1191–1208.
20. Aghdaei, S.; Sandison, M. E.; Zagnoni, M.; Green, N. G.; Morgan, H. Formation of Artificial Lipid Bilayers Using Droplet Dielectrophoresis. *Lab Chip* **2008**, *8*, 1617–1620.
21. Arnusch, A. J.; Branderhorst, H.; de Kruijff, B.; Liskamp, R. M. J.; Breukink, E.; Pieters, A. J. Enhanced Membrane Pore Formation by Multimeric/Oligomeric Antimicrobial Peptides. *Biochemistry* **2007**, *46*, 13437–13442.
22. Gennis, R. B. *Biomembranes: Molecular Structure and Function*; Springer: New York, 1989.
23. Tien, H. T; Ottova, H. L. *Membrane Biophysics*; Elsevier: Amsterdam, 2000.
24. Hille, B. *Ion Channels of Excitable Membranes*; Sinauer-Associates: Sunderland, 2001.
25. Tao, Z.; Toms, B. B.; Goodisman, J.; Tewodros, A. Mesoporosity and Functional Group Dependent Endocytosis and Cytotoxicity of Silica Nanomaterials. *Chem. Res. Toxicol.* **2009**, *22*, 1869–1880.
26. Ramachandran, S.; Kumar, G. L.; Blick, R. H.; van der Weide, D. W. Current Bursts in Lipid Bilayers Initiated by Colloidal Quantum Dots. *Appl. Phys. Lett.* **2005**, *86*, 083901.
27. Klein, S. A.; Wilk, S. J.; Thornton, T. J.; Posner, J. D. Formation of Nanopores in Suspended Lipid Bilayers using Quantum Dots. *J. Phys.: Conf. Ser.* **2008**, *109*, 012022.
28. Chen, J.; Hessler, J. A.; Putchakayala, K.; Panama, B. K.; Khan, D. P.; Hong, S.; Mullen, D. G.; DiMaggio, S. C.; Som, A.; Tew, G. N.; *et al.* Cationic Nanoparticles Induce Nanoscale Disruption in Living Cell Plasma Membranes. *J. Phys. Chem. B* **2009**, *113*, 11179–11185.
29. Dishon, M.; Zohar, O.; Sivan, U. From Repulsion to Attraction and Back to Repulsion: The Effect of NaCl, KCl, and CsCl on the Force between Silica Surfaces in Aqueous Solution. *Langmuir* **2009**, *25*, 2831–2836.
30. de Planque, M. R. R.; Raussens, V.; Contera, S. A.; Rijkers, D. T. S.; Liskamp, R. M. J.; Ruysschaert, J.-M.; Ryan, J. F.; Separovic, F.; Watts, A. β-Sheet Structured β-Amyloid-(1−40) Perturbs Phosphatidylcholine Model Membranes. *J. Mol. Biol.* **2007**, *368*, 982–997.
31. Kayed, R.; Sokolov, Y.; Edmonds, B.; McIntire, T. M.; Milton, S. C.; Hall, J. E.; Glabe, C. G. Permeabilization of Lipid Bilayers Is a Common Conformation-dependent Activity of Soluble Amyloid Oligomers in Protein Misfolding Diseases. *J. Biol. Chem.* **2004**, *279*, 46363–46366.
32. Lin, Y. S.; Haynes, C. L. Impacts of Mesoporous Silica Nanoparticle Size, Pore Ordering, and Pore Integrity on Hemolytic Activity. *J. Am. Chem. Soc.* **2010**, *132*, 4834–4842.
33. Le Bihan, O.; Bonnafous, P.; Marak, L.; Bickel, T.; Trépout, S.; Mornet, S.; De Haas, F.; Talbot, H.; Taveau, J. C.; Lambert, O. Cryo-electron Tomography of Nanoparticle Transmigration into Liposome. *J. Struct. Biol.* **2009**, *168*, 419–425.
34. Zhang, L.; Granick, S. How to Stabilize Phospholipid Liposomes (Using Nanoparticles). *Nano Lett.* **2006**, *6*, 694–698.
35. Wang, B.; Zhang, L.; Bae, S. C.; Granick, S. Nanoparticle-Induced Surface Reconstruction of Phospholipid Membranes. *Proc. Natl. Acad. Sci. U. S. A.* **2008**, *105*, 18171–18175.
36. Mornet, S.; Lambert, O.; Duguet, E.; Brisson, A. The Formation of Supported Lipid Bilayers on Silica Nanoparticles Revealed by Cryoelectron Microscopy. *Nano Lett.* **2005**, *5*, 281–285.
37. Rapuano, R.; Carmona-Ribeiro, A. M. Supported Bilayers on Silica. *J. Colloid Interface Sci.* **2000**, *226*, 299–307.
38. Roiter, Y.; Ornatska, M.; Rammohan, A. R.; Balakrishnan, J.; Heine, D. R.; Minko, S. Interaction of Nanoparticles with Lipid Membrane. *Nano Lett.* **2008**, *8*, 941–944.
39. Savarala, S.; Ahmed, S.; Ilies, M. A.; Wunder, S. L. Formation and Colloidal Stability of DMPC Supported Lipid Bilayers on SiO_2 Nanobeads. *Langmuir* **2010**, *26*, 12081–12088.
40. Ahmed, S.; Wunder, S. L. Effect of High Surface Curvature on the Main Phase Transition of Supported Phospholipid Bilayers on SiO_2 Nanoparticles. *Langmuir* **2009**, *25*, 3682–3691.
41. Chen, S. Y.; Cheng, K. H. Detection of Membrane Packing Defects by Time-Resolved Fluorescence Depolarization. *Biophys. J.* **1996**, *71*, 878–884.
42. Epand, R. M.; Epand, R. F. Lipid Domains in Bacterial Membranes and the Action of Antimicrobial Agents. *Biochim. Biophys. Acta* **2009**, *1788*, 289–294.